Theor Chim Acta (1988) 73: 337-364

Theoretica Chimica Acta

Extended Hartree–Fock (EHF) theory of chemical reactions*

III. Projected Møller–Plesset (PMP) perturbation wavefunctions for transition structures of organic reactions

K. Yamaguchi[1], Y. Takahara[1], T. Fueno[1], and K. N. Houk[2]

[1] Faculty of Engineering Science, Osaka University, Toyonaka, Osaka 560, Japan
[2] Department of Chemistry, University of California, Los Angeles, CA 90024, USA

(Received June 2, revised Ocober 5/Accepted October 9, 1987)

The triplet-instability analysis of the closed-shell RHF solutions has been carried out in relation to the orbital and spin correlation effects for various transition structures (TS) and reaction intermediates. It is found that the RHF solutions even for cyclic transition states of the Woodward-Hoffmann symmetry-allowed reactions often involve the triplet instability, indicating the crucial role of correlation corrections. The di- and tetra-radical characters for the transition structures are calculated by the projected UHF (PUHF) solutions resulting from the instability. The spin projection is also crucial for the UHF Møller-Plesset (UMP) correlated wavefunctions obtained for the transition structures of 1,3-dipolar, Diels-Alder, ene and related reactions. The relative stability between cyclic and acyclic TS for these reactions is examined at the approximately projected UHF MP2 (APU MP2) level. The former is found to be more favorable than the latter if the correlation correction is taken into account for TS in a well-balanced manner.

Key words: Triplet instability — Radical character — Spin projected UMP — Reaction mechanism — Transition structures

1. Introduction[1]

The closed-shell Hartree-Fock (RHF) solutions for transition states of organic reactions such as cycloadditions often involve the triplet-type (T) instability [1-3],

* Dedicated to Professor J. Koutecký on the occassion of his 65th birthday

[1] See Appendix B, p. 363, for notations

since the orbital and spin correlation effects are particularly important in such activated species. The more stable unrestricted Hartree-Fock (UHF) solutions result from the T-instability [4]. The energy gradient technique of the UHF solution has been used to locate transition structures of cycloaddition reactions [5]. The structures obtained by this procedure are often largely asynchronous even for the so-called Woodward-Hoffman symmetry-allowed reactions [6] such as 1,3-dipolar cycloadditions [7, 8] and Diels-Alder reactions [6, 9]. From these results and other thermochemical considerations, Dewar [6] has concluded that multibond reactions cannot normally be synchronous; however, Dewar's conclusion could be responsible for the spin contamination effect involved in singlet UHF solutions for transition structures (TS) [10] and/or for the correlation effects required for TS [11]. In this respect, a systematic theoretical analysis still remains an important problem.

In this series of papers [12, 13] (hereafter these are referred to as Parts I and II, respectively), symmetry-adapted wavefunctions obtained by the projection procedures for the generalized Hartree-Fock (GHF) solutions have been used to investigate the correlation and spin correlation effects for linear, Hückel and Möbius models of transition states and unstable intermediates; note that GHF solutions reduce to UHF or RHF solutions, depending on the type of the correlation effects [13]. The extended Hartree-Fock (EHF) solutions for these model systems have been obtained analytically to elucidate characteristics of the G(U)HF solutions, such as the spin projection and correlation effects on the potential curves [13]. It is found that the spin projection of the GHF solution is crucial even for qualitative discussions of properties such as a radical character for unstable species [13].

Recently, the Møller-Plesset (MP) perturbation theory has been successfully used as a method for simple computation of correlation energy [14]. The UHF MP (UMP) theory is quite acceptable for ordinary organic radicals [14]; however, it often involves a large spin contamination in transition states of organic radical reactions [15, 16]. Therefore, as a continuation of our previous work [12, 13], we examine here the projection procedures for the G(U)HF MP wavefunctions. It will be shown that the spin projection is crucial for the UMP wavefunctions responsible for cyclic and acyclic transition states of 1,3-dipolar cycloadditions [17, 18], Diels-Alder cycloadditions [10, 19] and ene reactions [21]. Implications of these results will be discussed in relation to the concerted and nonconcerted mechanisms for these reactions.

2. Theoretical backgrounds

2.1. Projected Møller-Plesset (MP) perturbation method

Previous symmetry and stability analyses [3, 4] have shown that the closed-shell HF (RHF) solutions for transition states often involve the triplet instability. Depending on the complexity of the correlation and spin-correlation effects, the stable HF solutions vary as follows:

$$\text{RHF} \rightarrow \text{UHF(ASDW)} \rightarrow \text{GHF(HSDW, HSW)}. \tag{1}$$

The UHF solution exhibits a one-dimensional (axial) spin-density modulation; this is referred to as the axial spin density wave (ASDW) solution [12, 13]. On the other hand, the GHF solutions have two- and three-dimensional spin density modulations: these are called helical spin density wave (HSDW) and helical spin wave (HSW) solutions respectively. As shown previously [13], RHF, UHF and GHF solutions can be characterized on the basis of the magnetic double point group theory.

Although GHF solutions can incorporate static or specific correlations arising from near orbital degeneracy and spin degeneracy [13], they involve no dynamical correlation. The MP perturbation method is effective for rapid computation of the correlation energy on the basis of the most stable HF solution reached from the instability analysis [13]:

$$\Psi_{\mathrm{GMP}} = \Psi_{\mathrm{GHF}} + \sum C_{ijk}^{abc} \Psi_{\mathrm{GHF}} \tag{2}$$

where Ψ_{GMP} and Ψ_{GHF} denote the GHF MP (GMP) and GHF wavefunctions, respectively. The second term (MP correction) in Eq. (2) involves the single, double, and other higher-order spin-unflip excitations from the ground GHF solution [13]. The GMP wavefunctions reduce to the UHF MP (UMP) or RHF MP (RMP) solutions in many "allowed" chemical reactions [14].

As discussed extensively in Part II [13], GHF solution [12–14] have intrinsic deficiencies such as spin symmetry-breaking properties; this error is not eliminated by the MP correlation correction, as has been pointed out for the UMP solution by Schlegel [16]. This may imply that the spin-symmetry breaking properties are attributable to the lack of spin-flip excitations in the GMP wavefunctions [13]. Therefore, the spin symmetry-projection is necessary for the GMP solution:

$$\Phi_{\mathrm{PGMP}} = \mathbb{P}_{\hat{\mathbb{S}}^2} \mathbb{P}_{\hat{\mathbb{S}}_z} \Psi_{\mathrm{GMP}} \tag{3}$$

where $\mathbb{P}_{\hat{\mathbb{S}}^2}$ and $\mathbb{P}_{\hat{\mathbb{S}}^2}$ have been defined as the projection operators responsible for the $\hat{\mathbb{S}}^2$- and $\hat{\mathbb{S}}_z$-spin eigenvalues [13].

Figure 1 illustrates schematically the computational scheme, where the triplet (T) and spin-flip (SF) instability conditions [4, 13] are utilized to determine the most stable HF solutions for the systems under consideration. For example, the GAUSSIAN 82 (G82) program package by Pople et al. [14] involves the STABLE [1] and MIX [4] subroutines for the T-unstable case; however, it does not yet provide the GHF solution for the SF-unstable UHF solution.

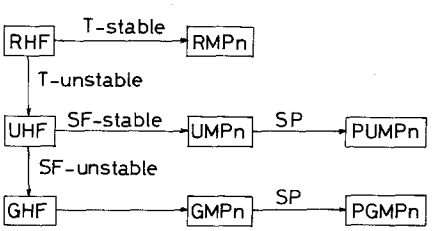

Fig. 1. A generalized Hartree-Fock (GHF) plus Møller Plesset (MP) perturbation method followed by the spin projection (SP). T and SF mean the triplet and spin-flip instability conditions for the RHF and UHF solution respectively

Recently, Schlegel [15] has shown that the fourth-order UMP (UMP4) energy for transition states of free radical additions is greatly improved by the use of Lowdin's single annihilation procedure. This is usually reliable enough for acyclic free radicals as examined by Schlegel [13, 15], although the single annihilation approximation breaks down for transition structures examined here, since two bonds are largely spin-polarized. In fact, the $\langle \mathbb{S}^2 \rangle$-values after the single annihilation (see LINK 502 in G82 [14]) become larger than the corresponding values before annihilation. The full projection is desirable for the spin symmetry as well as the size-consistency condition, although it is time-consuming.

2.2. Approximate projection procedure

Instead of the full spin projection for the UMP wavefunction, we consider here an approximate projection procedure which satisfies the size-consistency condition [14]. The nth order UMP (UMPn) wavefunctions for acyclic radical species with the spin eigenvalue S usually involve the (S+1) component as a spin contaminant [15]:

$$^{(2S+1)}\Psi(\mathrm{UMPn}) = C_{2S+1}\,{}^{(2S+1)}\Phi(\mathrm{PUMPn}) + C_{2S+3}\,{}^{(2S+3)}\Phi(\mathrm{PUMPn}) \tag{4}$$

where $^{(2S+m)}\Phi(\mathrm{PUMPn})$ and C_{2S+m} denote, respectively, the nth order projected UMP (PUMPn) wavefunction and its coefficient for the (2S+m) spin state. In order to calculate the energy of the pure (2S+1) spin state from Eq. (4), we need the energy of the pure (2S+3) spin state. We assume that the $^{(2S+3)}$UMPn wavefunction does not involve any significant amount of spin contamination,

$$^{2S+3}\langle \mathbb{S}^2 \rangle(\mathrm{PUMPn}) \cong {}^{2S+3}\langle \mathbb{S}^2 \rangle(\mathrm{UMPn}), \tag{5}$$

in which case the following relationship is expected for the corresponding total energies:

$$^{2S+3}\mathrm{E}(\mathrm{PUMPn}) \cong {}^{2S+3}\mathrm{E}(\mathrm{UMPn}). \tag{6}$$

Under this assumption [22, 23], the approximate PUMPn energy is given by

$$^{2S+1}\mathrm{E}(\mathrm{APUMPn}) = {}^{2S+1}\mathrm{E}(\mathrm{UMPn}) + f_{sc}[{}^{2S+1}\mathrm{E}(\mathrm{UMPn}) - {}^{2S+3}\mathrm{E}(\mathrm{UMPn})], \tag{7}$$

where $^{2S+m}\mathrm{E}(\mathrm{APUMPn})$ and $^{2S+m}\mathrm{E}(\mathrm{UMPn})$ denote the total energies of the APUMPn and UMPn energies respectively. The fraction of the spin contamination is given by the total spin angular momenta, which are calculated by the UMP solutions [22] to be

$$f_{sc} = [{}^{2S+1}\langle \mathbb{S}^2 \rangle(\mathrm{UMPn}) - \mathrm{S}(\mathrm{S}+1)]/[{}^{2S+3}\langle \mathbb{S}^2 \rangle(\mathrm{UMPn}) - {}^{2S+1}\langle \mathbb{S}^2 \rangle(\mathrm{UMPn})], \tag{8}$$

where S(S+1) is the exact total spin angular momentum for the (2S+1) spin state.

Several spin couplings are conceivable for the lowest spin (LS) state of cyclic transition structures with more than three-unpaired electrons [12, 13]. For example, a cyclic TS with four radical electrons has two different singlet spin coupling schemes I and II, as shown in Fig. 2. The axial spin structures I and II can be described by UHF solutions with different magnetic symmetries [13]. If I and II are nearly degenerate in energy, the UHF solutions become SF-unstable,

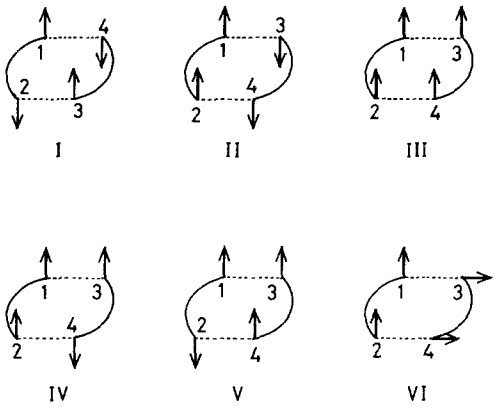

Fig. 2. Spin vector models of possible spin couplings for four-orbital-four-electron (4, 4) systems (see text)

being reorganized into a more stable GHF solution which is approximately given by a linear combination of the UHF I and II solutions [13]. Furthermore, there are one quintet configuration (III) and three triplet spin configurations (IV-VI) with spin states III-V given by UHF and VI by GHF [13]. This indicates that a large number of UHF and GHF solutions with intermediate spin (IS) state are available for polyradical systems.

To avoid handling a large number of IS states, use the highest-spin (HS) UMPn solution for the approximate spin projection of the lowest-spin (LS) G(U)MP solution:

$$^{LS}E(APGMPn) = {}^{LS}E(GMPn) + f_{sc}[{}^{LS}E(GMPn) - {}^{HS}E(UMPn)] \quad (9)$$

$$f_{sc} = [{}^{LS}\langle \mathbb{S}^2 \rangle (GMPn) - S(S+1)]/[{}^{HS}\langle \mathbb{S}^2 \rangle (UMPn) - {}^{LS}\langle \mathbb{S}^2 \rangle (GMPn)], \quad (10)$$

where the HS state is usually described by the UMP wavefunction. The second term in Eq. (9) is the effective exchange integral (J_{eff}) derived previously by the combination of projected HF and the Heisenberg model [22]. This in turn indicates that the present spin projection for the LS state of polyradicals is accomplished under the assumption that the energy splittings among the LS, IS and HS states are given by the Heisenberg model plus spin projected MP theory [22]. As shown by comparison with CI results, this is a useful approximation to the full spin projection given by Eq. (4). Needless to say, the full projection [13] would be necessary for more accurate estimations of the spin projection energy [22, 23].

3. Triplet instability analysis for intermediates and transition structures

3.1. General consideration and radical character

Let us first consider bond-breaking and bond-forming processes, represented as functions of a common reaction coordinate (q) [6]. There are in principle two different cases (A) and (B) under the HF molecular orbital (MO) approximation, as illustrated in Fig. 3. The triplet instability for the closed-shell HF (RHF) solution occurs at a certain stage of the bond-breaking process, and therefore

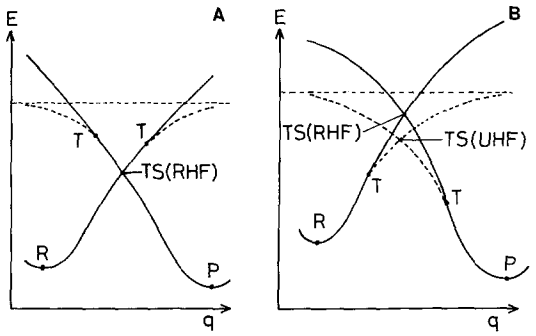

Fig. 3. Potential curves for bond interchange processes. The transiton structures (TS) are located in the T-stable and T-unstable regions in cases A and B respectively

the transition structure for a bond-interchange process can be described within the RHF solution as shown in Fig. 3A if the potential curve crossing occurs outside the triplet (T)-unstable region. On the other hand, the RHF solution is T-unstable at the curve crossing point, i.e. the transition structure, in Fig. 3B, indicating the existence of the more stable UHF TS with some degree of diradical (DR) character. The same situation is also expected for unstable reaction intermediates with DR characters.

The DR character, y_d, is defined by the orbital overlap between the split HOMOs for up- and down-spins (ψ^+ and ψ^-) related to a bond dissociation [4]:

$$y_{HO} = 1 - 2T_{HO}/(1 + T_{HO}^2), \tag{11}$$

where

$$T_{HO} = \langle \psi^- | \psi^+ \rangle. \tag{12}$$

The DR character may also be written in terms of the deviation ΔS^2 of the $\langle \mathbb{S}^3 \rangle$ values from the exact one, $S(S+1)$, by using the relation (see Appendix)

$$\Delta S^2 = {}^{2S+1}\langle \mathbb{S}^2 \rangle (\mathrm{UHF}) - S(S+1) = 1 - T_{HO}^2 \tag{13}$$

in which case

$$y_d = 1 - 2\sqrt{1 - \Delta S^2}/(2 - \Delta S^2). \tag{14}$$

Figure 4 illustrates the functional dependence of y_d upon the ΔS^2-value, together with the variation in the normalized spin density [4]:

$$\rho = \sqrt{\Delta S^2}. \tag{15}$$

Two bond-forming (breaking) processes occur during the course of cycloaddition reactions, as illustrated by the spin coupling (I and II) in Fig. 2. Therefore, the TS exhibit a more or less tetraradical (TR) character, y_t, if the so-called resonance stabilization for TS are insufficient. y_t is simply defined by an equation of the same form as Eq. (11), although the ΔS^2-values given by the UHF solution are divided by two in this case, since these are responsible for the breaking of two bonds (see appendix); therefore, the DR character is given by $2y_t$. The TR character should be enhanced for acyclic TS because of a loss of resonance stabilization.

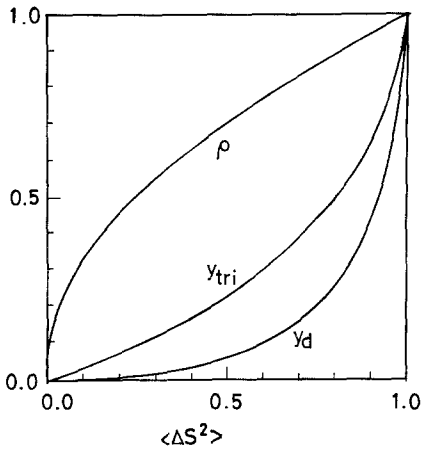

Fig. 4. Variation of diradical (y_d) and triradical (y_{tri}) characters and normalized spin density ρ against the deviation ΔS^2 of total spin angular momentum from the exact value S(S+1)

3.2. Triplet instability analysis

The triplet instability analysis of the RHF 3-21G solution was carried out for reaction intermediates as well as cyclic and acyclic TS that had been determined by several groups [5-11, 15-21]. Table 1 summarizes the lowest eigenvalues (λ_0) of the triplet instability matrices for several TS. The corresponding UHF 3-21G solutions were also constructed by the orbital-mixing procedure [4, 14] in the triplet unstable case, and DR and TR characters were calculated on the basis of Eqs. (13) and (14). Table 2 summarizes the ΔS^2 and $y_d(y_t)$-values for TS.

The triplet instability for several reactants was examined first. The RHF solution was triplet-stable ($\lambda_0 > 0$) for organic molecules such as ethylene and acetylene, indicating no DR character within the HF MO approximation [4]. Similarly, fulminic acid (HCNO) is a 1,3-dipolar species without DR character. On the other hand, the DR characters of ozone and carbonyl ylide were calculated to be 33% and 25%, respectively, by the UHF 3-21G method. The oxygenated dipoles are regarded as 1,3-dipoles with moderate DR

Table 1. The lowest eigenvalues (λ_0) of the triplet instability matrices for RHF 3-21G solutions for transition structures

Types of reactions	Systems	Ts	λ_0(eV)
1,2-rearrangement reactions	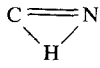	CTS(**1**)	0.66
		CTS(**2**)	1.06
1,3-dipolar cycloadditions	HCNO+HC≡CH	CTS(**10**)	−0.86
	HCNO+HC≡CH	NTS(**11**)	−3.38
	$O_3+CH_2=CH_2$	CTS(**12**)	−5.56
	$CH_2OCH_2+CH_2=CH_2$	CTS(**14**)	−3.10
Ene reaction	$CH_3CH=CH_2+CH_2=O$	CTS(**18**)	0.49

Table 2. Total spin angular momenta and radical characters for transition structures from the UHF and PUHF 3-21G methods

Types of reactions	Systems	TS	$\langle S^2 \rangle$		
			b.a.	a.a.	$y_d(y_t)(\%)$
1,3-dipolar cycloaditions	$HCNO+HC\equiv CH$	CTS(**10**)	0.66	0.78	4 (2)
		NTS(**11**)	1.49	4.23	38 (19)
	$O_3+CH_2=CH_2$	CTS(**12**)	1.11	1.24	16 (8)
	$O_3+CH_2=CH_2$	NTS(**13**)	1.38	2.78	30 (15)
	$CH_2OCH_2+CH_2=CH_2$	CTS(**14**)	1.02	1.24	12 (6)
Diels-Alder reaction	$CH_2=CH-CH=CH_2+CH_2=CH_2$	CTS(**16**)	0.97	1.73	10 (5)
	$CH_3CH=CH_2+CH_2=CH_2$	CTS(**18**)	0.38	0.17	3[b]
Ene reaction	$CH_3CH=CH_2+O_2$	CTS(**20**)	1.15	1.38	18 (9)[b]

[a] b.a. and a.a. denote before and after single spin annihilation
[b] Value using the 6-31G* basis set

characters, which is consistent with the result of the GVB [24] treatment as well as our previous results [4].

As shown previously [25], the transition state for the symmetry-allowed disrotatory opening of oxirane exhibits a moderate DR character because of the DR character of carbonyl ylide

$$\text{oxirane} \rightarrow \text{TS with DR character} \rightarrow \overset{\delta\cdot}{C}H_2\cdots O\cdots\overset{\delta\cdot}{C}H_2 \tag{16}$$

On the other hand, there is no triplet instability for the transition structures [26] of 1,2-rearrangement reactions of H_2CN^+, as shown in Table 1, implying that the DR character is zero for these ionic TS. The situation could be similar for other 1,2-cationic rearrangement reactions as well.

Interestingly, the RHF solution becomes triplet-unstable for the essentially cyclic transition states [27] in the 1,3-dipolar cycloaddition of fulminic acid to acetylene. The situation is the same for transition structures of other 1,3-dipolar cycloadditions: ethylene plus ozone [17] and ethylene plus carbonyl ylide [18]. However, while the TR character is rather large for the acyclic TS [11] of the 1,3-dipolar cycloaddition between fulminic acid and acetylene, it is not so large for those cyclic TS examined here.

The RHF 3-21G solution is also triplet-unstable for several six-orbital six-electron transition structures for the Diels-Alder reaction between butadiene and ethylene [10], 1,5-sigmatripic rearrangement of 1,3-pentadiene [19] and ene reaction between propene and ethylene [21]; however, the TR characters are calculated to be generally weak. Moreover, it disappears in the case of TS for ene reaction between propene and formaldehyde because of the introduction of ionicity by the hetero atom (oxygen). On the other hand, the TR character is not negligible for TS of the ene reaction between singlet oxygen and propene, because of the DR character of singlet oxygen.

The triplet instability of the RHF 3-21G (6-31G*) solutions for cyclic transition structures of the Woodward-Hoffmann allowed reactions [28] is not so surprising since the correlation and spin correlation effects are more or less important for such unstable structures, as recognized from Fig. 3. Since the resulting singlet UHF solutions involve the higher-spin contamination terms, the DR and TR characters might be considered to be very large if the spin density and ΔS^2-values themselves were utilized as criteria for the radical character. However, it is noteworthy that the radical character defined by the spin-projected UHF (PUHF) solution is a slowly increasing parameter compared with the ΔS^2 value (see Fig. 4), in accord with the UHF natural orbital (NO) CI [29] and EHF [13] results.

4. Spin projection for the UMP wavefunctions

4.1. Spin projection for the singlet UMPn *solution*

We first examine the reliability of the approximation PUMPn (APUMPn) method for singlet species with comparison of the CI results. The extensive CI calculations have been carried out for the 1,2-hydrogen migration reactions in carbenes and

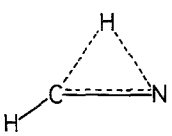

1

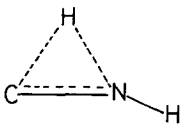

2

other related species. As an example, the isomerization of the H_2CN^+ molecular ion is examined here. The MP4 6-31G* calculations were performed for the linear $HCNH^+$ ion, two different TS (**1**, **2**) and intermediates CNH_2^+ and $N^+{=}CH_2$. Table 3 summarizes the relative energies obtained by the RMP4 and APUMP4

Table 3. Relative energies for the CNH_2^+ ions by the RMP4 and CI methods

	E_{rel}	
System	MP4	CI[a]
$HCNH^+$	0.0[b]	0.0
$C{\equiv}NH_2^+$	52.2	46
	51.4[c]	
$N^+{=}CH_2$	74.5	72
	74.4[c]	
$HC{=}N^+$ (**1**) 	61.7	61
$C{=}NH$ (**2**) 	76.8	76

[a] [26]
[b] −93.4565 a.u.
[c] APUMP4 results

methods, together with those of the CI method [26], and it can be seen that all three methods provide similar results for these ions; this indicates the reliability of the MP perturbation method. The APUMP4 method gives slightly smaller relative energies for $C{=}NH_2^+$ and $N^+{=}CH_2$ as compared with the RMP4 method.

Ozone and carbonyl ylide were studied as unstable intermediates with moderate DR characters. The singlet (S) and triplet (T) gap ΔE_{ST} were calculated for comparison with CI as

$$\Delta E_{ST} = {}^{HS}E({}^3UMPn) - {}^{LS}E(X), \tag{17}$$

where X denotes the ^{1}RMPn, ^{1}APUMPn or ^{1}UMPn method, and the results are summarized in Table 4. The ST gap calculated for ozone by the APUMP4 method is close to the best GVB CI [30] and experimental values [31], while the UMP4 value is about one-half of them. This clearly indicates the necessity of the spin projection for the singlet UMPn wavefunction. On the other hand, the RHF

Table 4. Energy differences between the lowest (LS) and highest (HS) spin states by the MPn 6-31G* method

System	Method	$\Delta E_{LS\text{-}HS}(n)$				
		1	2	3	4	Others
$CH_2{-}CH_2$	RMP	−71.2	−29.7	−30.4	−20.8	
($\sigma\pi$-DR)	APUMP	5.47	2.14	1.75	1.62	1.82[a]
	UMP	2.66	1.05	0.86	0.80	
O_3	RMP	−38.3	61.4	28.9	50.5	37[b]
($\pi\pi$-DR)	APUMP	19.0	40.9	34.9	43.9	39[c]
	UMP	10.4	23.0	19.6	24.7	
CH_2OCH_2	RMP	−38.5	20.6	11.2	20.0	
($\pi\pi$-DR)	APUMP	8.91	18.6	16.5	20.2	
	UMP	4.78	10.2	9.01	11.1	
CH_2CH_2O	APUMP	4.36	3.21	3.15	3.19	
($\sigma\sigma$-Dr)	UMP	1.62	1.48	1.46	1.48	
CH_2CHCH_2	APUMP	244	236	236	236	
(π-R)	UMP	226	224	224	224	
CH_2CHO	APUMP	99.1	122	117	120	
(π-R)	UMP	93.1	117	112	115	
$CH_2(CH)_3CH_2$	APUMP	157	144[d]			
(π-R)	UMP	132	127[d]			
$CH{-}CHCH_2$	APUMP	238	232	232	232	
($\sigma\pi$-DR)	UMP	223	221	221	221	
$CH{-}CHO$	APUMP	98	122	116	121	
($\sigma\pi$-DR)	UMP	93	118	113	117	

[a] CI [32]
[b] CI [30]
[c] Exp. [31]
[d] 3-21G value

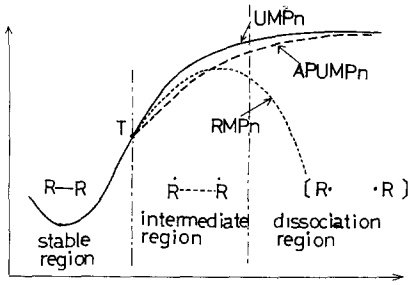

Fig. 5. Typical potential curves for dissociation processes obtained by the RHF, UHF and APUHF MP calculations

method gives the negative ST gap, as has already been emphasized by Goddard [24], while the ST gap from the RMP4 method is 10 kcal/mol larger than the experimental value. This may be attributable to an overestimation of the stability of the ground singlet state of ozone by the RMP4 method (see Fig. 5). The RMPn and APUMPn ($n \geq 2$) methods provide similar ST gaps for carbonyl ylides while the UMPn value is about one-half of the corresponding PUMPn value; the situation could be similar in other oxygenated dipoles with moderate DR characters [4].

Bismethylene and C-O cleaved oxirane, i.e, $\sigma\pi$-DR, were examined as examples with very strong DR characters. The ST gaps for bismethylene are largely negative in sign for the RMPn method, indicating the breakdown of the approximation, whereas for the APUMPn ($n \geq 2$) method they are close to that of the multi-reference (MR) CI method [32]. On the other hand, the UMPn value is about one-half the APUMPn value since it involves the triplet contamination[2]. The ST gap for the $\sigma\sigma$-DR state of CH_2CH_2O is positive in sign as in the case of a free radical dimer, for example, the methyl radical dimer.

In summary, the RMPn method is applicable to unstable species with a small DR character, both the RMPn and APUMPn calculations are desirable for species with intermediate DR characters, since the reliability of these methods is largely dependent on characteristics of systems under consideration, and the APUMPn method is preferable for unstable species with strong DR character, since the RMPn method often breaks down in the bond-dissociation region. The RMPn energy exhibits an oscillation around the exact value with the order n of the perturbation expansion [15]. Figure 5 illustrates a typical feature of the potential curve determined from the dissocation reaction of a covalent bond by the RMPn, UMPn, APUMPn and PUMP [16] calculations.

4.2. Spin projection for doublet and triplet UMPn *wavefunctions*

The spin contamination for doublet UMPn wavefunction is not so serious in most cases, although it often is for conjugated free radicals [13]. For example the $\langle \mathbb{S}^2 \rangle$-values for allyl and formylmethyl radicals are 0.97 and 1.09 respectively

[2] We thank Professor J. A. Pople for helpful discussion on the spin contamination for the UMPn wavefunction for bismethylene at Hawaii meeting, 1984

by the ^{2}UHF method. The triradical character for free radicals is defined as previously [33]

$$y_{tri} = 2(1 - \sqrt{1 - \Delta S^2})/[3 - \Delta S^2] \tag{18}$$

where $\Delta S^2 = \langle \mathbb{S}^2 \rangle_{UHF} - 0.75$.

Figure 4 illustrates the variation of y_{tri} against the ΔS^2-value; the triradical characters for these species are calculated to be small 8% and 14% respectively, but these values are significant relative to the energies between the doublet and quartet spin states. The energy gap between the LS and HS states is defined as

$$\Delta E_{LS\text{-}HS} = {}^{HS}E({}^{HS}UMPn) - {}^{LS}E(X), \tag{19}$$

where X denotes the ^{LS}UMPn or ^{LS}APUMPn method; Table 4 summarizes the energy gaps obtained. The doublet states of allyl and formylmethyl radicals are stabilized by about 12 and 5 kcal/mol respectively after the spin projection at the UMP4 level. Thus the closed-shell pair for tricentric free radicals are more or less pin-polarized. This is consistent with previous EHF results for the three-center three-electron (3, 3) model [13], indicating that the complete active space SCF (CASSCF) with the (3, 3) active space is desirable at the multi-configuration (MCSCF) level: note that the EHF wavefunction is equivalent to the CASSCF one for the (3, 3) system.

The UHF MOs for spin-polarized singlet pairs in open-shell species are generally given by [33]

$$\psi_i^{\pm} = \cos\theta\phi_i \pm \sin\theta\phi_i^* \tag{20}$$

where ϕ_i and ϕ_i^* are the spatially symmetry-adapted natural orbitals (NOs). Since the ϕ and ϕ^* NOs for the allyl radical have the same b_1-symmetry, its doublet UHF solution satisfies the C_{2v} spatial symmetry, although it is spin-symmetry broken. Consequently the fully optimized structure of allyl radical by the UHF energy gradient technique is C_{2v}-symmetry adapted, in contrast to those of bond-alternating ^{2}RHF (NRHF) [33, 34] and spatially symmetry-broken MCSCF wavefunctions [35, 36]. Figure 6 shows the orbital mixings due to the spin polarization (SP) mechanism in the UHF solution. The spatial symmetry for the ^{2}UHF solution is satisfied in case A, while it is broken in case B. Therefore the UHF energy gradient technique permits the fully optimized molecular structures with and without spatial symmetry for A and B, respectively.

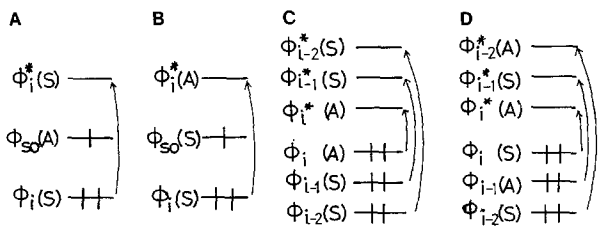

Fig. 6A–D. Orbital mixing schemes in the UHF solution. The spatial symmetry of the UHF solution is conserved in cases **A** and **C**, while it is broken in cases of **B** and **D**

Recent *ab initio* MCSCF studies [37] have shown that the transition state for Cope rearrangement exhibits a weak DR character. The TS for the Cope and Claisen rearrangements could be regarded, respectively, as the dimerized state of allyl radicals and the coupled state between allyl and formylmethyl radicals.

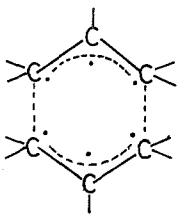

3

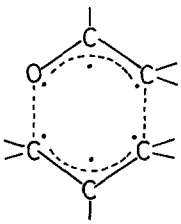

4

Judging from the free radical stabilizations by spin projection in Table 4, the APUMPn treatments of TS should be used at the MP level, as discussed elsewhere [38]. The fully optimized structure of the TS for Cope rearrangement by the UHF method is C_s-symmetry adapted, with the orbital mixings given by Fig. 6C. On the other hand, Osamura et al. [37] have shown that the two-configuration MCSCF treatment is inappropriate in this case. The APUMP2 results indicate that the CASSCF with the six-orbital six-electron (6, 6) active space could be necessary for reliable treatments of the TS at the MCSCF level.

The situation is similar in the case of [1, n] signatropic reactions, whose TS are regarded as the coupled states of the conjugated free radicals and hydrogen atom as follows [39]. If the bonding interactions between radical fragments are weak, the RHF solutions should be T-unstable; in fact, the TS for the 1,5-hydrogen

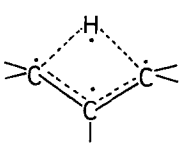

5

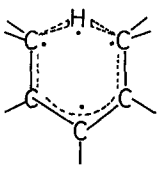

6

migrations correspond to this case although the reactions are formally symmetry-allowed. According to Houk et al. [40], the $\langle \mathbb{S}^2 \rangle$-values by the singlet UHF solutions are 1.3 and 0.8 for the C_{2v} and C_s TS respectively, so that the DR characters for these TS are 24% and 6%, respectively. These TS by the UHF solutions should be C_s symmetry-adapted since the orbital mixings are as depicted in Fig. 6C.

Vinyl and formylmethylenes were considered as examples of triplet conjugated radicals. The $\langle \mathbb{S}^2 \rangle$-values are 2.18 and 2.13 respectively at the UMP2 6-31G* level,

and the energy gains in the ground state after spin projection are 10.4 and 4.0 kcal/mol respectively; these are not at all trivial for the triplet (LS) and quintet (HS) energy gap, as shown in Table 4. As will be shown later, the spin projection is also essential at transition states for the addition of triplet radicals to double bonds.

In summary, the spin projection is crucial for the UMPn wavefunctions for open-shell conjugated radicals, since the spin polarizations of π-bonds are relatively large. The energy gain by this procedure is significant for relative energies such as the LS–HS gap.

5. Spin projection and correlation effects for the symmetry allowed reactions

5.1. Additions of monocentric diradicals to olefins

The addition of monocentric DRs (^{1}O, ^{1}NH, etc.) to double bonds are regarded as the symmetry-allowed reactions in the sense of Woodward and Hoffman [28]. As an example, the addition of an oxygen atom to ethylene to form oxirane is examined here. Figure 7 illustrates the energy diagram obtained for two different reaction paths by the second-order MP 6-31G* method. The ST gap for the O-atom by the APUMP2 method is 52 kcal/mol, whereas it is about one-half of this from the unprojected UMP2 method. The former value is incompatible with

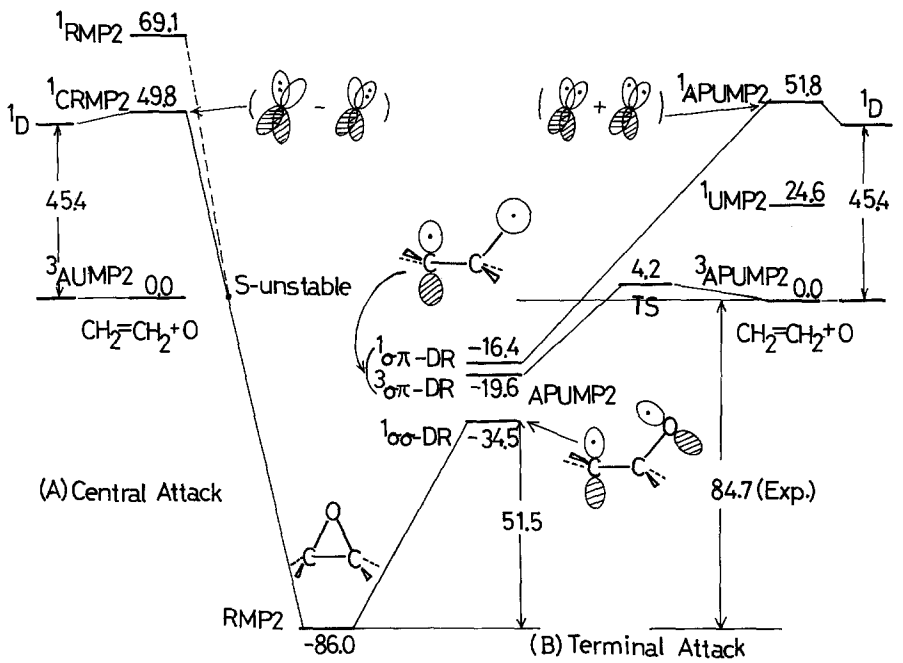

Fig. 7. Energy diagrams for the central (A) and terminal (B) attacks of atomic oxygen on ethylene calculated with the RHF, UHF and PUHF MP 6-31G* methods

the experimental value of the ^3P-^1D gap. A complex RMP2 (CRMP2) wavefunction arising from the off-diagonal singlet instability [4] is also available for the ^1D state of O, and this yields an ST gap of 50 kcal/mol, in agreement with experiment. However, the APUMP and CRMP wavefunctions provide apparently different orbital descriptions of the ^1D state of O, i.e., the out-of-phase combination of the closed-shell configurations and the complete DR configuration respectively, as illustrated in Fig. 7. Therefore, two different reaction paths are conceivable for the addition of O to ethylene: the central attack (A) given by CRMP2, and the terminal attack (B) given by APUMP2. The former path can provide the closed-shell product directly, i.e., oxirane, since CRMP2 reduces to RMP2 at the singlet (S)-instability threshold as illustrated in Fig. 7. On the other hand, the latter path correlates with the singlet DR intermediate, since APUMP2 describes the DR configuration with A″ symmetry. Neither the central nor terminal attack of $O(^1D)$ to ethylene has an energy barrier.

The activation barriers for the terminal attack of $^3O(^3P)$ to ethylene are calculated by the UMP2 and APUMP2 methods to be 10.2 and 4.2 kcal/mol respectively. The reduction of activation energy by spin projection is remarkable, as was the case for the free radical additions investigated by Schlegel [15]. The APUMP2 value is compatible with the experimental value (1.5 kcal/mol). The energy lowering on going from the ^3O plus ethylene system to oxirane is 86 kcal/mol, in agreement with the experimental heat change (85 kcal/mol).

Singlet molecular oxygen has the $^1\Delta$ state which is analogous to the ^1D state of O. The central attack of $^1O_2$ to the C-C double bond gives a perepoxide (PE)-like TS, while the terminal attack provides the $\sigma\sigma$ (or $\sigma\pi$) DR-like TS; these reaction paths are described by CRMP2 and APUMP2, respectively. The total energies for PE- and $\sigma\sigma$-DR TS calculated from these methods with a 6-13G* basis set (BS) are −228.1450 a.u. and −228.1405 a.u. respectively. Therefore, PE TS(**7**) is 2.8 kcal/mol more stable than $\sigma\sigma$-DR TS(**8**). According to the CASSCF CI calculations by Roos et al. [41], the corresponding energy difference is 4.7 kcal/mol, supporting the MP2 result; however, our preliminary APUMP2 calculations show that the $\sigma\pi$-DR TS(**9**) without the C_s symmetry is much more stable than the symmetry-restricted PE TS(**7**). Extensive computations beyond the MPn level will be necessary for exact determinations of relative energies of **7**–**9** [38].

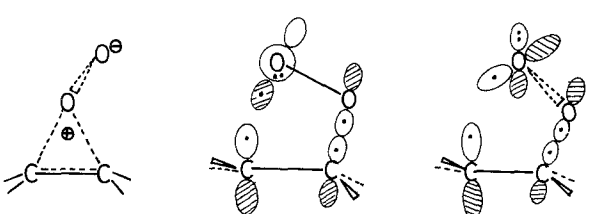

7 8 9

5.2. 1,3-dipolar cycloadditions

The mechanism of 1,3-dipolar cycloadditions is still controversial. For the cycloaddition of 1,3-dipoles to ethylene, Dewar et al. [7] have proposed a noncyclic transition state (NTS) by the MINDO/2 method, whereas Komornicki et al. [27] have reported a cyclic TS (CTS) on the basis of the RHF CI with the double zeta (DZ) plus polarization (P) BS. Hiberty et al. [11] have determined the NTS by the UHF energy gradient and RHF 3×3 CI techniques. The geometries obtained for the TS are similar, although the former solution is spin-symmetry broken. Hiberty et al. have investigated the relative stability between CTS and NTS on the basis of two-reference restricted MP (TRMP) perturbation method. It was found that within the TRMP2 4-31G approximation. the CTS(**10**) is less stable than the NTS(**11**) for the 1,3-dipolar cycloaddition between fulminic acid and acetylene. Their result is in contradiction to the Woodward-Hoffmann symmetry-rule and the observed stereochemistry for 1,3-dipolar cycloadditions [42]. Here, the RMP2 and APUMP2 6-31G* calculations were carried out for both the TS determined by Komornicki et al. [27] and Hiberty et al. [11]. The energy diagrams obtained are illustrated in Fig. 8.

From Fig. 8, CTS(**10**) is more stable than NTS(**11**) within the RHF approximation, since it does not take the electronic correlation into account. The situation is reversed in the case of the UHF approximation, in accord with Dewar's MINDO/2 result, because it partly incorporates the correlation correction arising from the near orbital degeneracy [13]. The stability of NTS(**11**) is increased after spin projection, namely at the APUHF level. The activation barrier for the 1,3-dipolar cycloaddition by the APUHF method is negative in sign, since the RHF solutions for the reactants involve no correlation. Therefore, the dynamical correlation correction is crucial even for qualitative discussion of the reaction mechanism.

The activation barrier for CTS(**10**) is calculated to be 21 kcal/mol by the APUMP2 method, which is close to the RHF CI (DZP) result (19 kcal/mol) obtained by Komornicki et al. [27]. This in turn indicates the reliability of the approximation given by Eq. (9). On the other hand, the RMP2 method underestimates the barrier heights for CTS(**10**) in comparison with the RHF CI (DZP). Interestingly, CTS(**10**) is more stable by about 10 kcal/mol than NTS(**11**) at the APUMP2 level. The same tendency is recognized for the UMP2 result, although the situation is reversed at the RMP2 level, in accord with the TRMP approximation by Hiberty et al. [11]. This may be attributable to the fact that the RMPn approximation breaks down in the case of unstable species with a strong DR character as illustrated in Fig. 5.

The present APUMP2 results support the concerted mechanism for the 1,3-dipolar cycloaddition between fulminic acid and acetylene. This is consistent with the observed stereochemistry for typical 1,3-dipolar cycloadditions; however, the present results are not yet conclusive. For quantitative discussions of the relative stability between CTS(**10**) and NTS(**11**), we feel that at least two implementations are necessary: (1) the full geometry optimizations of both CTS(**10**) and NTS(**11**)

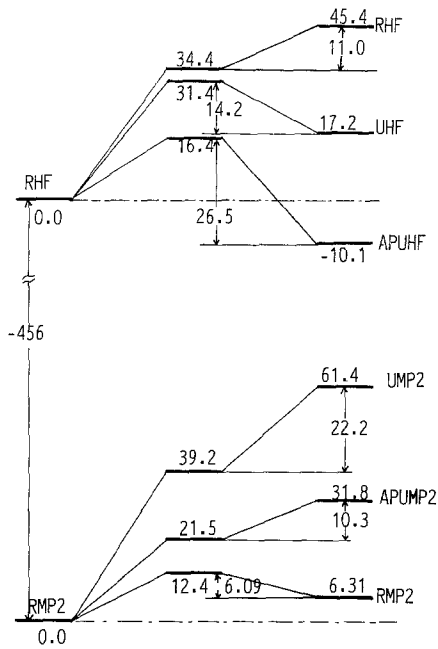

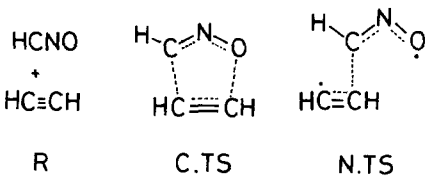

Fig. 8. Relative stability between cyclic (CTS) and noncyclic (NTS) transition structures for the fulminic acid plus actylene system calculated with the RHF, UHF and APUHF MP2 6-31G* methods

by the APUMP2 energy gradient technique and (2) the correlation correction by the APUMP4 method or by the projected UHF coupled-cluster (CC) method. The energy difference between them probably becomes less than 10 kcal/mol after these refinements, i.e., PUMP4//PUMP2 and/or APUMP4//APUMP2.

Both the RMP2 and APUMP2 6-31G* calculations were carried out for the 1,3-dipolar cycloadditions between ethylene and oxygenated dipole (ozone or carbonylylide). The cyclic transition structure for the ozone plus ethylene system was determined by the RHF 4-31G energy gradient technique, while that for the carbonylylide plus ethylene system is taken from the literature [18]; Table 5 summarizes the activation barriers obtained. From Table 4, the barrier heights for CTS(**12**) of the ethylene plus ozone system are about 16 kcal/mol, 15 kcal/mol and −16 kcal/mol at the RHF, UHF and APUHF levels respectively. The APUHF underestimates the activation barrier, since it partly involves the correlation correction for the transition structure with a considerable DR character. These barriers become about 15 kcal/mol, 30 kcal/mol and 10 kcal/mol respectively by the RMP2, UMP2 and APUMP2 methods. The APUMP2 value is about twice the experimental estimation (5 kcal/mol) [17].

Table 5. Activation energies for transition structures using the MP2 6-31G* method

Reactions	Type	Methods						
		RHF	UHF	APUHF	RMP2	UMP2	APUMP2	Ref.
$O_3+CH_2=CH_2$	CTS(**12**)	15.7	14.6	−16.2	14.7	30.0	10.0	5[a]
$CH_2OCH_2+CH_2=CH_2$	CTS(**14**)	61.5	80.7	64.9	66.3	87.0	72.2	
Butadiene+$CH_2=CH_2$[b]	CTS(**16**)	38.3	33.0	30.9	19.2	33.3	28.5	28[c],34[d]
	NTS(**17**)	99.3	63.8	55.4	74.5	73.6	58.9	
Propene+$CH_2=CH_2$	CTS(**18**)	65.5	64.0	51.9	51.9	67.8	53.4	
Propene+$CH_2=O$	CTS(**20**)	54.2	—	—	32.9	—	—	

[a] Exp. [17]
[b] 3-21G values
[c] Exp. [44]
[d] Exp. [45]

The activation barriers for the 1,3-dipolar cycloaddition between carbonyl ylide and ethylene are particularly large when compared with those of the ozonolysis reactions. The full optimization of CTS(**14**) by the RHF or APUHF energy gradient technique is necessary for the further refinements of the MP2 activation energies.

The relative energy between CTS and NTS for the 1,3-dipolar cycloadditions of oxygenated dipoles with olefins is a subtle problem. Judging by the APUMP2 results for fulminic acid, the energy differences between CTS and NTS are less

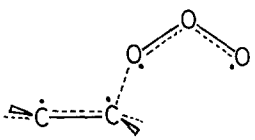

NTS(13)

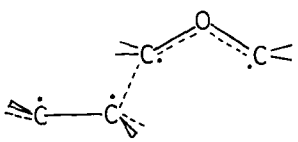

NTS(15)

than 10 kcal/mol for these reactants, since (1) ozone and carbonylylide have moderate DR characters and (2) the radical characters are relatively large even for CTS (**12**, **14**). The PUMP4//PUMP2 treatments of both CTS(**12**, **14**) and NTS(**13**, **15**) are desirable for further quantitative discussions of their energy differences.

5.3. Diels–Alder reactions

Dewar et al. [5] have shown that the TS for the Diels–Alder reaction between butadiene and ethylene is noncyclic at the MINDO/3 UHF level. Since the orbital mixings in the UHF solution are as depicted in Fig. 6D, the spatial symmetry of the UHF solution for Diels–Alder reaction is broken; consequently their results are not at all surprising. On the other hand, Houk et al. [10] have reported the cyclic synchronous TS determined for the reaction by the RHF 3-21G energy gradient technique, and have concluded that the reaction is concerted, in combination with the observed stereochemistry [10]. Independently, Bernardi et al. [19]

have obtained stereochemistry [10]. Independently, Bernardi et al. [19] have obtained the same conclusion by the CASSCF 4-31G calculations. Salem et al. [43] have shown that the energy difference between CTS(**16**) and NTS(**17**) is only 2–4 kcal/mol by the RHF(4-31G) 3 × 3 CI method. Here, the RMP2 and UMP2 3-21G calculations have been carried out for CTS(**16**) by Bernardi et al. [19], and NTS(**17**) by Salem et al. [43]. The results are summarized in Table 5.

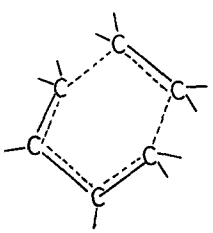

CTS (16)

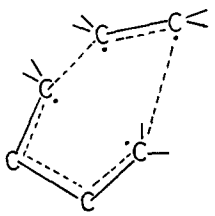

NTS (17)

The RHF 3-21G solution is T-unstable for cis-butadiene with the optimized geometry by the two-configuration (TC) MCSCF method; this indicates the important role of electronic correlation for polyenic systems. The activation barriers for the CASSCF TS were calculated by the RHF, UHF and APUHF approximations to be about 38 kcal/mol, 33 kcal/mol and 31 kcal/mol respectively. The RHF result agrees with that (38 kcal/mol) obtained by Houk et al., although the CASSCF TS [19] is different from the RHF TS [10]. On the other hand, the corresponding barriers become 19 kcal/mol, 33 ckal/mol and 29 kcal/mol for the RMP2, UMP2 and APUMP2 methods. The UMP2 and APUMP2 values are in the experimentally estimated range of 28–34 kcal/mol for the activation barrier of the Diels–Alder reaction [44, 45]. The RMP2 method underestimates the barrier since it overestimates the stability of CTS(**16**) with a moderate radical character.

From Table 5 the CTS(**16**) of Bernardi et al. [19] is more stable than the NTS(**17**) of Salem et al. [43] by about 30 kcal/mol within the APUMP2 approximation; the same tendency is recognized for the RMP2 result. The energy gaps between CTS(**16**) and NTS(**17**) by both the APUMP2 and RMP2 methods seem too large, since the geometry of NTS(**17**) is only partially optimized by the RHF 3 × 3 CI method. The PUMP4/PUMP2 refinements of both CTS(**16**) and NTS(**17**) are desirable for further quantitative discussion of the energy difference between them.

5.4. Ene reactions and other Woodward–Hoffman allowed reactions

Loncharich and Houk [21] have determined the transition structures for ene reactions of propene with ethylene, formaldehyde and singlet oxygen at the RHF 3-21G level. Assuming their geometries, the activation energies for the ene reaction between propene and ethylene were calculated by both the RMPn and APUMPn 6-31G* methods; the results are summarized in Table 5. It is apparent that both

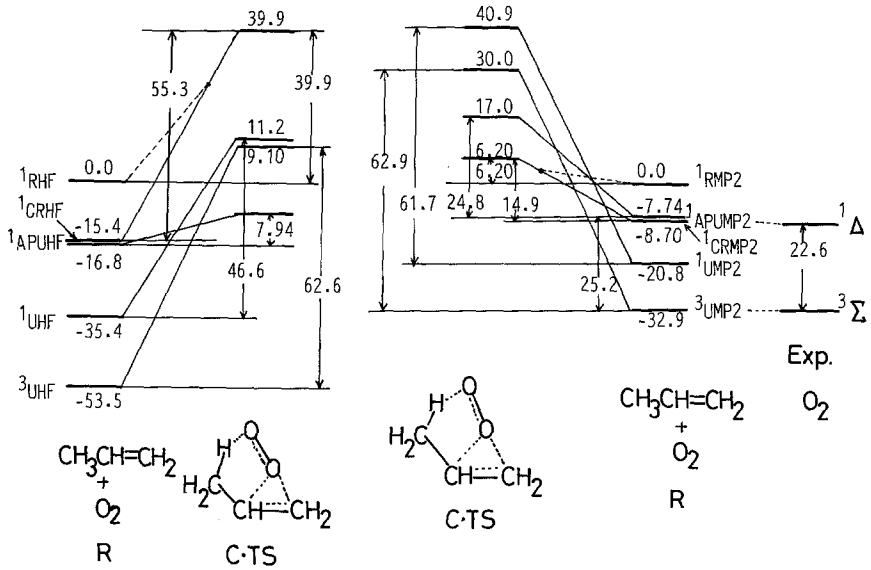

Fig. 9. Energy diagrams for ene reaction between propene and singlet oxygen at the SCF (A) and MP2 (B) 6-31G* levels

the RHF and UHF methods provide similar activation barriers for CTS(**18**). On the other hand, the barrier of the PUHF method is about 10 kcal/mol lower than the other two; however the APUMP2 and RMP2 predict similar activation barriers. These results indicate that the radical character is weak in the case of ene reactions between closed-shell species.

Figure 9 illustrates the energy diagrams for the ene reaction between propene and singlet oxygen. The APUMPn and CRMPn energies for $^1O_2$ are nearly degenerate in energy, being responsible for the $^1\Delta$ state. The cyclic TS(**20**) results from the latter approximation. Activation barriers for CTS(**20**) are about 55 kcal/mol, 47 kcal/mol and 8 kcal/mol, respectively, at the CRHF, UHF and APUHF level, which implies that the nonconcerted TS(**21**) is feasible if the UHF energy gradient technique is used to locate the transition structure of this reaction.

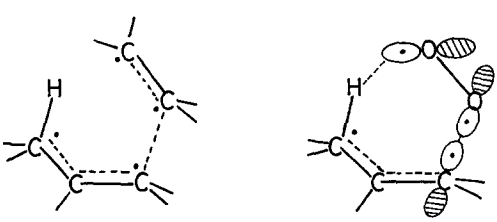

NTS(19) NTS(21)

The preceding results for the 1,3-dipolar and Diels-Alder reactions indicate that NTS(**21**) could be more stable than CTS(**20**) at the UHF and APUHF level, and this situation is reversed at the APUMP2 and UMP2 levels because of the well-balanced correlation corrections for both TS. The activation barriers for CTS(**20**) of the ene reaction between propene and singlet oxygen are about 15 kcal/mol, 62 kcal/mol and 25 kcal/mol respectively, at the CRMP2, UMP2 and APUMP2 levels.

There are other symmetry-allowed reactions such as electrocyclic reactions of polyenes. The RHF solutions for the TS of these reactions are probably T-unstable since the correlation effects for polyenic systems are significant. Nevertheless, the logical extension of the present analysis may lend support to the concerted mechanism for these symmetry-allowed reactions as well as other related Woodward-Hoffman allowed reactions if the correlation corrections for TS are taken into account in a well-balanced manner.

6. Discussion and concluding remarks

6.1. Electronic correlation effects for potential curves

The *ab initio* RHF solutions are triplet (T) unstable for singlet unstable molecules such as oxygenated dipoles, being compatible with previous semiempirical calculations [4, 25]. The more stable UHF solutions for 1,3-dipoles are spatially symmetry-broken since the symmetry and mixing of natural orbitals are as shown in Fig. 6D, and the spatial symmetry restriction is therefore relaxed for the species under the UHF approximation. As an example, the full geometry optimizations of carbonyl ylide were performed assuming both the symmetrical and unsymmetrical geometries as trials and the same C_{2v} symmetry-adapted geometry resulted from both computations. This means the C_{2v} structure for carbonyl ylide is more stable than other broken-symmetry structures even within the UHF SCF approximation, which includes the specific orbital correlation.

The present results shed light on a general feature of the potential curves for the Woodward-Hoffmann symmetry-allowed reactions. The RHF and RMPn potential curves are useful enough for the location of concerted transition states (TS) without significant radical characters. On the other hand, the UHF and APUHF potential curves often provide the nonconcerted TS with strong radical characters. At the HF SCF level, the TS by UHF are usually more stable than the RHF TS, since the UHF solution takes into account the specific orbital correlation effects for singlet pairs with DR characters, while the RHF energy involves no correlation energy. However, nonconcerted mechanisms for "allowed" reactions deduced by the UHF and APUHF calculations are not compatible with the observed sterochemistry [10, 39].

Such failures at the HF SCF level can be easily removed if the correlation corrections are taken into account for both TS in a well-balanced manner. The APUMPn method includes a qualitatively correct feature of potential curves as

illustrated in Fig. 7, since it includes such corrections by the perturbation procedure. Therefore, both UMP2 and APUMP2 calculations correctly predict concerted mechanisms for the Woodward-Hoffmann allowed reactions examined here.

From these results, it seems probable that the ab initio HF MP results can be reproducible at the semiempirical MNDO level if appropriate correlation corrections are added. One such approach is the second-order Brillouin-Wigner perturbation theory with the Epstein-Nesbet (BWEN) method based on the MNDO approximation as proposed by Thiel [46].

6.2. Symmetry and stability analysis of organic reaction

Previously [2], we classified electronic mechanisms of organic reactions into four types on the basis of the orbital symmetry and triplet instability criterion for the RHF solution. In this paper we have examined several kinds of organic reactions. These results enable us to depict the generalized MO (GMO) correlation diagrams, which are responsible for the four reaction mechanisms proposed previously [2]; Fig. 10 illustrates typical orbital correlation diagrams.

The symmetry-allowed nonradical (AN) mechanism in Fig. 10 corresponds to the Woodward-Hoffmann symmetry-allowed concerted mechanism [28], but it does not rule out the possibility of the nonsynchronous but concerted TS discussed by Dewar [6]; CTS(**20**) for the singlet oxygen ene reaction is one such example. The AN reaction requires conservation of the orbital-phase continuity and bonding interaction between the reaction sites. As has already been pointed out by Dewar from the MINDO/3 results [6], the DR character is not negligible even for various concerted reactions via a formally AN mechanism [21]; in this regard,

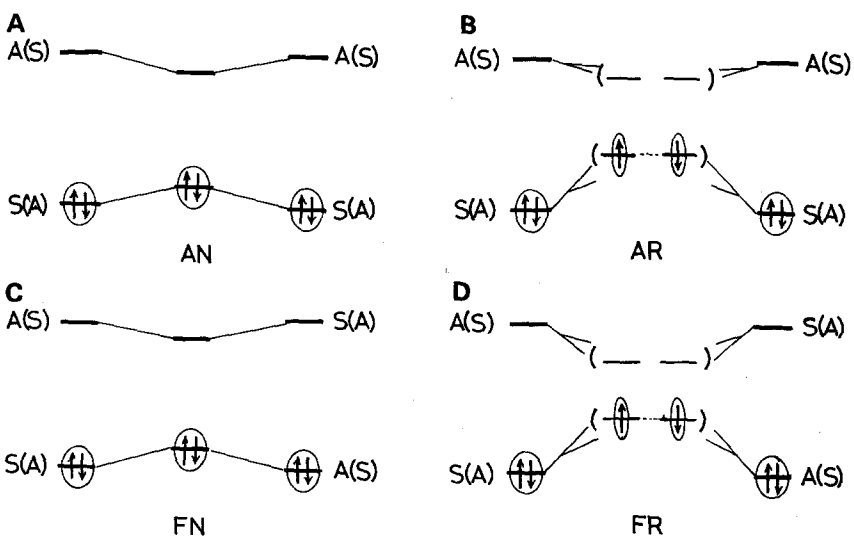

Fig. 10A–D. Orbital correlation diagrams for four different reaction mechanisms on the basis of the orbital symmetry and stability criteria (notations are given in text)

Dewar has first revealed the crucial role of electronic correlations for organic TS within the semiempirical MO approximation. The *ab initio* UHF 6-31G* results indicate that the radical character is also non-negligible for the examined here. *Ab intio* UHF and UHF calculations predict greater stability for a two-step path via a noncyclic TS (NTS) than for a one-step concerted path in these reactions, in accord with Dewar's MINDO/3 UHF results. This is attributable to the fact that the UHF and APUHF wavefunctions partly include the correlation corrections for TS with radical character. It is noteworthy that the spin contamination effect is not a major factor giving NTS in the UHF theory [10].

According to the APUMP2 6-31G* results, CTS is more favorable than NTS for several symmetry-allowed reactions examined here, in lien with the observed stereochemistry and other evidence. This implies that the dynamical correlation correction is crucial for a well-balanced estimation of relative energy between CTS and NTS. The APUMP2 method is one of such computational technique. On the other hand, use of the RMPn method should be made with care since it greatly overestimates or underestimates the stability of NTS with a strong DR character (see Fig. 5), although the RHF solution itself always favors a CTS with a weak DR character as has been shown by Houk et al. [10]. The present theoretical results lend support to the original closed-shell picture for concerted reactions by Woodward and Hoffman as illustrated in Fig. 10A, although the orbital correlations given by Fig. 10B are certainly non-negligible for TS.

The DR characters for TS are significant for formally symmetry-allowed diradical (AR) reactions. Since molecular oxygen is the ground-triplet species, the energy difference between the AN and AR TS could be particularly small. The retro Diels-Alder reactions of endoperoxides of anthracene derivatives probably proceed through the AR mechanism, since the reaction modes are sensitive to the external magnetic field, indicating the generation of short-lived DR intermediate as follows [47]:

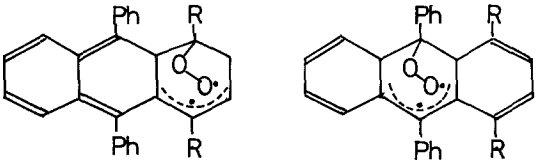

The present APUMP2 calculations also suggest the possibility of a nonconcerted TS for the (2+2) cycloaddition between singlet molecular oxygen and ethylene [47]. Thus the theoretical distinction between AR and AN is important for a full understanding of the symmetry-allowed reactions illustrated in Fig. 10B.

The symmetry-forbidden DR (FR) mechanism corresponds to the symmetry-forbidden nonconcerted mechanism of Woodward and Hoffman [28] and include thermal decompositions of dioxetanes and dioxetanones. The FR reactions appear to involve strong spin-orbit coupling between singlet and triplet DR and the magnetic field effect for the spin inversion. On the other hand, the DR characters for TS and short-lived intermediates are largely reduced in the case of nonradical

ionic reactions, even though they are formally characterized as symmetry-forbidden; these reactions are of the FN type. The substituents, polar solvents, gegen ions, and catalysts are found to be effective for the transitions from DR to zwitterions [48]. For example, such neutral radical-zwitterionic transition is important for understanding the BF_3-catalyzed ring-opening of dioxetanes.

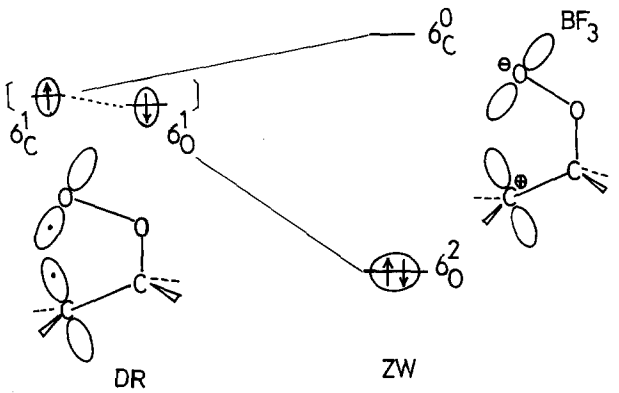

Thus, orbital symmetry, orbital stability and orbital splitting are of particular importance in discriminating organic reaction mechanisms in the ground state as illustrated in Fig. 10C and D.

6.3. The onset region for covalent-bond instability

Schlegel [16] has shown that the projected fourth-order Møller–Plesset (PUMP) perturbation correction almost smoothes out the cusp on the potential curve by PUHF at the onset of the RHF/UHF instability; this was essentially the same for the approximate PUMPn (APUMPn) method. Therefore the cusp problem is not so serious for the PUMPn and APUMPn wavefunctions; however, it is a limitation for very accurate computation of the potential curves near the onset of the covalent-bond instability using these methods. The more reliable beyond-HF theories such as CI and coupled-cluster (CC) methods are desirable for such a purpose, as is briefly discussed in Appendix A. Bearing this limitation in mind, we can apply the UMPn and PUMPn methods to various chemical problems. They will be published elsewhere [38], together with detailed numerical data for the present systems under consideration. Very recently, Kahn et al. [49] have shown that the optimized geometries of 1,3-dipoles by the ^{1}UHF 6-31G* method are in good agreement with the experimental results. Judging from their results, the transition structures determined by the 3-21 basis set should be significantly improved by the use of the 6-31G* basis set.

6.4. Concluding remarks

Judging from the present results, the HF MP procedures followed by the spin projection are useful for qualitative studies of organic reaction mechanisms in

the ground state. Electronic correlation corrections by the MP method are of practical importance for determination of relative stability between concerted and nonconcerted TS. The procedures employed here are summarized as follows:

1. Location of a cyclic TS (CTS) by the singlet RHF energy gradient technique.

2. Examination of the triplet instability of the RHF solution for CTS.

3. Determination of the more stable singlet UHF solution for CTS if the RHF solution is T-unstable.

4. Location of a noncyclic TS (NTS) by the UHF energy gradient technique.

5. Calculation of radical characters for CTS and NTS by the PUHF wavefunctions, and drawing of the orbital correlation diagrams for them by the use of RHF and PUHF MOs.

6. Calculation of the RMPn and APUMPn energies for CTS, and calculation of the APUMPn energy for NTS.

7. Calculation of activation energy for CTS by both RMPn and APUMPn, and calculation of the activation energy for NTS by APUMPn.

8. Calculation of the energy difference between CTS and NTS by APUMPn.

9. Comparison between computational results and experiments.

The present results may indicate that the projected HF MP treatments (1)-(9) provide reliable conclusions in most cases. Where the results indicate the necessity of further quantitative calculations, the following computations beyond HF MP level should be added:

10. Relocation and identification or improvement of CTS and NTS geometries by the PUMPn energy gradient technique.

11. Recalculation of the energy difference between CTS and NTS by the CAS MBPT or MR CC method.

Acknowledgements. This work was supported by the Joint Studies Program (1986-1987) of the Institute of Molecular Science (IMS). We thank Professor K. Nasu for his kind help and advice.

Appendix A

The canonical UHF orbitals are transformed into the corresponding orbitals [50] to determine the UHF natural orbitals in Eq. 20. The total spin angular momentums for the UHF solutions are given by

$$\langle \mathbb{S}^2 \rangle = S(S+1) + \sum_{i}^{Nb} [1 - S_i^2] \tag{A1}$$

where S is given by the difference between the numbers of the up (N_a) and down (N_b) spins, and S_i is the orbital overlap between the corresponding MOs for a singlet pair, where

$$S = 1/2(N_a - N_b), \qquad S_i = \langle \psi_i^+ | \psi_i^- \rangle \tag{A2}$$

The split singlet pairs can be selected from the magnitudes of the orbital overlaps. For example, except for the split HOMOs the orbital overlaps are almost 1.0 in the case of DR species [4]. On the other hand, two singlet pairs are largely spin-polarized in the case of transition structures with TR characters. The natural orbitals for these pairs are transformed into the localized natural orbitals (LNO) [51] to define the split bond orbitals which are responsible for the TR character as shown in the text.

The spin projection is necessary for all the split singlet pairs, which have smaller orbital overlaps than 1.0 [4] in contrast to the single spin annihilation [15, 16]. The natural orbitals responsible for these split pairs are taken as the complete active orbitals for our CAS treatment of unstable molecules. The PUHF can be obtained as a by-product of full CI within the CAS for all the split pairs as shown previously [52]. The correlation diagrams for the ground and lower excited states,

$$\Phi(\text{CAS CI}) = \sum D_i \Phi_i \quad (\text{full CI within CAS}) \tag{A3}$$

can be given by the CAS MR CI combined with the perturbation selection of configurations [52]. On the other hand, the dynamical correlation corrections can be calculated in a size-consistent manner by the many-body perturbation (MBPT) or the coupled-cluster (CC) method starting from the CAS CI wavefunctions for split pairs as shown previously [53]. In this sense, the present PUMP method is one alternative for the CAS MBPT using UHF NOs [53].

The derivatives of the APUMP energy (Eq. 9) are useful for re-locations of transition structures. To obtain the first derivative of the total energy,

$$\begin{aligned} \partial^{\mathrm{LS}}\mathrm{E}(\mathrm{APUMP})/\partial q = {} & \partial^{\mathrm{LS}}\mathrm{E}(\mathrm{UMP})/\partial q + f_{\mathrm{sc}}[\partial^{\mathrm{LS}}\mathrm{E}(\mathrm{UMP})/\partial q - \partial^{\mathrm{HS}}\mathrm{E}(\mathrm{UMP})/\partial q] \\ & + \partial f_{\mathrm{sc}}/\partial q[{}^{\mathrm{LS}}\mathrm{E}(\mathrm{GMP}) - {}^{\mathrm{HS}}\mathrm{E}(\mathrm{UMP})], \end{aligned} \tag{A4}$$

the first derivative of the total spin angular momentum is needed. This can be written in terms of the MO coefficient and its first derivative:

$$\partial\langle \$^2 \rangle/\partial q = \left(\sum_{m_i}^{\text{all}} U_{mi}^q s_{mj} + \sum_{m}^{\text{all}} V_{mj}^q S_{im} \right) + \sum_{\mu} \sum_{\nu} C_{\mu}^i C_{\nu}^i S_{\mu\nu}^q \tag{A5}$$

where S_{mj} and C_{μ}^i denote, respectively, the orbital overlap between the canonical UHF MOs and the MO coefficient. The elements U_{mi}^q and V_{mj}^q of the first derivatives are determined by the use of the coupled-perturbed HF method used for computations of the second derivatives of the UHF energy. Therefore, the energy gradient for APUMP may be obtained from the GAUSSIAN 82 program package [14] without significant program change.

Appendix B

Many abbreviations are used in this paper. The notations for computational methods are given as follows:

HF:	Hartree-Fock	RHF:	restricted HF
NRHF:	bond-alternating RHF	CRHF:	complex RHF
EHF:	extended HF	UHF:	unrestricted HF
PUHF:	projected UHF	ASDW:	axial spin density wave
HADW:	helical spin density wave	HSW:	helical spin wave
MPn:	Møller-Plesset *n*-th order	CC:	coupled cluster

The notations for electronic and transition structures are given as follows:

S:	singlet	T:	triplet
LS:	lowest spin	HS:	highest spin
IS:	intermediate spin	SF:	spin flip
SP:	spin polarization	DR:	diradical
TR:	tetraradical	TS:	transition structures
CTS:	cyclic TS	NTS:	noncyclic TS
AN:	symmetry-allowed nonradical	AR:	symmetry-allowed diradical
FN:	symmetry-forbidden nonradical	FR:	symmetry-forbidden diradical

References

1. Čížek J, Paldus J (1967) J Chem Phys 47:3976
2. Yamaguchi K, Fueno T, Fukutome H (1973) Chem Phys Lett 22:461
3. Bonačič-Koutecký V, Koutecký J (1975) Theor Chim Acta 36:149
4. Yamaguchi K (1975) Chem Phys Lett 33:330; (1975) 35:230
5. Dewar MJS, Olivella S, Rzepa HS (1978) J Am Chem Soc 100:5650
6. Dewar MJS (1984) J Am Chem Soc 106:209
7. Dewar MJS (1977) Discuss Faraday Soc 62:197
8. Lluch JM, Bertran J (1979) Tetrahedron 35:2601
9. Dewar MJS, Pierini AB (1984) J Am Chem Soc 106:203
10. Houk KN, Lin Y-T, Brown FK (1986) J Am Chem Soc 108:554
11. Hiberty PC, Ohanessian G, Schlegel HB (1983) J Am Chem Soc 105: 719
12. Yamaguchi K, Yoshioka Y, Fueno T (1977) Chem Phys Lett 46:360
13. Yamaguchi K, Yoshioka Y, Takatsuka K, Fueno T (1978) Theor Chim Acta 48:185
14. Hehre WJ, Radom L, Schleyer PVR, Pople JA (1986) *Ab-initio* molecular orbital theory. Wiley, New York
15. Sosa C, Schlegel HB (1986) Int J Quantum Chem 29:1001
16. Schlegel HB (1986) J Chem Phys 84:4530
17. Leroy G, Sana M (1976) Tetrahedron 32:1379
18. Leroy G, Nguyen, M-T, Sana M (1976) Tetrahedron 32:1529
19. Bernardi F, Bottoni A, Robb MA, Field MJ, Hilger IH, Guest MF (1985) J Chem Soc Chem Commun 1051
20. Hess BA Jr, Schaad LJ, Pancir J (1985) J Am Chem Soc 107:149
21. Loncharich RJ, Houk KN: to appear in J Am Chem Soc
22. Yamaguchi K, Fukui H, Fueno T (1986) Chem Lett 625
23. Yamaguchi K, Jensen F, Dorigo A, Houk KN: Chem Phys Lett, in press

24. Wadt WR, Goddard III, WA (1975) J Am Chem Soc 97:3004
25. Yamaguchi K, Fueno T (1973) Chem Phys Lett 23:471
26. Schaefer HF (1979) Acc Chem Res 12:288
27. Komornicki A, Goddard JD, Schaefer III HF (1980) J Am Chem Soc 102:1763
28. Woodward RB, Hoffmann R (1969) Angew Chem Int Ed 8:781
29. Yamaguchi K, Yabushita S, Fueno T, Kato S, Morokuma K, Iwata S (1980) Chem Phys Lett 71:563
30. Hay PJ, Dunning Jr, TH (1977) J Chem Phys 67:2290
31. Swanson N, Celotta, RJ (1975) Phys Rev Lett 35:783
32. Buenker RJ, Peyerimhoff SD (1976) Chem Phys 9:75
33. Yamaguchi K, Fueno T (1976) Chem Phys Lett 38:47
34. Paldus J, Veilard A (1978) Mol Phys 35:445
35. Kikuchi O (1980) Chem Phys Lett 72:487
36. McLean AD, Lengsfield III, BH, Pacansky, J, Ellinger Y (1985) J Chem Phys 83:3567
37. Osamura Y, Kato S, Morokuma K, Feller D, Davidson ER, Boden WT (1984) J Am Chem Soc 106:3362
38. Yamaguchi et al., to be published
39. Jensen F, Houk KN: J Am Chem Soc, in press
40. Bernardi F, Robb MA, Schlegel HB, Tonachini G (1984) J Am Chem Soc 106:1198
41. Hottokka M, Roos B, Siegbahn P (1983) J Am Chem Soc 105:5263
42. Huisgen R (1963) Angew Chem Int Ed 2:565, 633
43. Townshend RF, Ramunni G, Segel G, Hehre WJ, Salem L (1976) J Am Chem Soc 98:2190
44. Rowley D, Stein H (1951) Discuss Faraday Soc 10:198
45. Uchiyama M, Tomioka T, Amano (1964) J Phys Chem 68:1878
46. Thiel W (1981) J Am Chem Soc 103:1413
47. Yamaguchi K (1985) In: Frimer AA (ed) Singlet oxygen, vol III. CRC Press, Boca Raton, FL
48. Yamaguchi K, Yabushita S, Fueno T (1981) Chem Phys Lett 78:566
49. Kahn SD, Hehre WJ, Pople JA (1987) J Am Chem Soc 109:1871
50. Amos AT, Hall GG (1961) Proc Roy Soc A263:483
51. Yamaguchi K, Ohta K, Fueno T (1977) Chem Phys Lett 50:266
52. Yamaguchi K, Iwata S (1980) Chem Phys Lett 76:375
53. Yamaguchi K (1980) Int J Quantum Chem S14:269